

Biological effects of extracorporeal shockwave in bone healing: a study in rabbits

Ching-Jen Wang · Feng-Sheng Wang ·
Kuender D. Yang

Received: 31 July 2007 / Published online: 17 June 2008
© Springer-Verlag 2008

Abstract

Introduction This study is an investigation of the biological effects of extracorporeal shockwave treatment (ESWT) on bone healing in a rabbit model.

Materials and methods Sixteen 12-month-old New Zealand white rabbits with body weight ranging from 2.5 to 3.5 kg were used in the study. An intra-medullary pin was inserted retrograde into the femur canal. A closed fracture of the femur was created with a three-point bend method. The animals were randomly divided into the study group and the control group with eight rabbits in each group. The study group received shockwave treatment, whereas the control group did not. The animals were killed at 12 weeks, and a 5-cm long femur bone including the callus was harvested. The specimens were subjected to biomechanical study, histomorphological examination, and immunohistochemical analysis.

Results The shockwave group showed significantly better bone strength in biomechanical study, more cortical bone formation in histomorphological examination and higher number of neo-vessels and angiogenic and osteogenic

growth markers including VEGF, eNOS, PCNA, and BMP-2 on immunohistochemical stains than the control group.

Conclusion ESWT significantly improved bone healing after fracture of the femur in rabbit. ESWT promoted the formation of cortical bone what might have been associated with increased biomechanical results. ESWT-promoted bone healing was associated with increased neovascularization and up-regulation of angiogenic and osteogenic growth factors.

Keywords Shockwave · Bone healing · Biological effect · Rabbits

Introduction

Extracorporeal shockwave treatment (ESWT) was shown effective in non-union of long bone fracture with a success rate ranging from 65 to 85% [3, 9–14]. The positive effect of shockwave in promoting bone healing was demonstrated in both acute fracture and chronic non-union in animal experiments [2, 4, 6, 7, 15]. Despite the success in clinical application and the positive effect in animal study, the exact mechanism of shockwave in bone healing remains unknown. Recently, ESWT was shown to induce the ingrowths of neovascularization and increased angiogenic growth factors at the Achilles tendon-bone junction in dog and rabbit models [17, 20]. We hypothesized that shockwave-promoted bone healing may show similar biological effects. The purpose of this study was to investigate the efficacy of shockwave in bone healing and to unveil the working mechanism through the biological effects of shockwave-promoted bone healing in rabbits.

C.-J. Wang (✉)

Department of Orthopedic Surgery,
Chang Gung Memorial Hospital,
Chang Gung University College of Medicine,
123 Ta-Pei Road, Niao-Sung Hsiang,
Kaohsiung 833, Taiwan
e-mail: w281211@adm.cgmh.org.tw

F.-S. Wang · K. D. Yang

Department of Medical Research,
Chang Gung Memorial Hospital,
Chang Gung University College of Medicine,
Kaohsiung, Taiwan

Materials and methods

The Institutional Review Board of our hospital approved the study. The animal experiments were performed under the guidelines and the care and use of animals in research. Sixteen New Zealand white rabbits, 12 months old, with body weight ranging from 2.5 to 3.5 kg were used in this study. The rabbits were anesthetized with intra-muscular ketamine (25 mg/kg) and phenobarbital (30 mg/kg). The right lower limb was scrubbed and draped in surgically sterile fashion. A mini-arthrotomy of the knee was made through a medial parapatellar incision. A drill hole was made at the center of the intercondylar notch, and a 2.0 mm Kirschner pin was inserted retrograde into the canal of the femur. The proximal end of the pin was exited through a separate incision over the trochanter, and the tip of the pin was bent to prevent it from migration. The distal end of the pin was cut flush with the articular surface of the distal femur condyles. The incisions were closed in routine fashion after irrigation with normal saline.

A closed fracture of the right femur was created with a three-point bend method [5]. The hip and knee were supported on a three point bending apparatus, and a closed fracture of the right femur was created at the mid-third with a loading anvil. Special care was undertaken to avoid bending of the intra-medullary pin when the fracture occurred. The fracture was confirmed with radiographic examination (Fig. 1). Postoperative prophylaxis included ampicillin (50 mg/kg) every 12 h given intramuscularly for 5 days. The rabbits were kept in the housing cage and cared for by a veterinarian. The surgical wounds, the alignment and stability of the fractured limb and the overall activities of the rabbit were monitored daily.

The rabbits were randomly divided into two groups with eight rabbits in the study group and eight in the control group. The study group received 2,000 impulses of shockwaves at 20 kV (equivalent to 0.47 mJ/mm² energy flux density) to the fracture site in 1 week after the fracture when the surgical wounds had healed. The source of shockwave was from an electrohydraulic OssaTron (Sanuwave, Alpharetta, GA, USA). The fracture site and the depth of treatment were confirmed with the control guide of the machine under C-arm imaging. Surgical lubricate was placed onto the skin in contact with the shockwave tube. ESWT was applied in two planes at 90° with 1,000 shocks in each plane as a single session. Immediately after the treatment, the affected limb was inspected for local redness, swelling, or hematoma. The control group received no shockwave. The rabbits were returned to the housing cages with no additional immobilization.

Serial radiographs of the right femur in A-P and lateral views were performed at 1, 4, 8 and 12 weeks. The fracture



Fig. 1 Radiographs of the right femur in anteroposterior and lateral views showed fracture of the femur with an intra-medullary pin fixation

healing was evaluated by clinical assessment and confirmed with radiographs. Clinical assessments included local tenderness and motion at the fracture site. Radiographs evaluated the amount of callus formation and the bridging bone across the fracture site. All fractures healed radiographically in 12 weeks.

The rabbits were killed at 12 weeks. The K-pin was removed and a 5-cm long segment of the femur bone including the callus was harvested. The bone specimens were subjected to biomechanical study, histomorphological examination, and immunohistochemical analysis.

Biomechanical study

The bone strength tests including peak load, peak stress, and modulus of elasticity were performed using a slow load compression test on Material Testing System OT 10 (MST Corp., Minneapolis, MN). A supporting apparatus with two supporting points 30 mm apart was placed on the stage of the machine. The specimens were tested on a supported beam using an actuator displacement rate of 2 mm/min. To avoid rotation of the bone during testing, the bending load was applied to the concave surface of the femur bone. The press head was rounded off to avoid cutting into the bone when loaded. The fracture load (lb) and the deflection of bone (mm) were read from the load–deflection curve (Fig. 2).

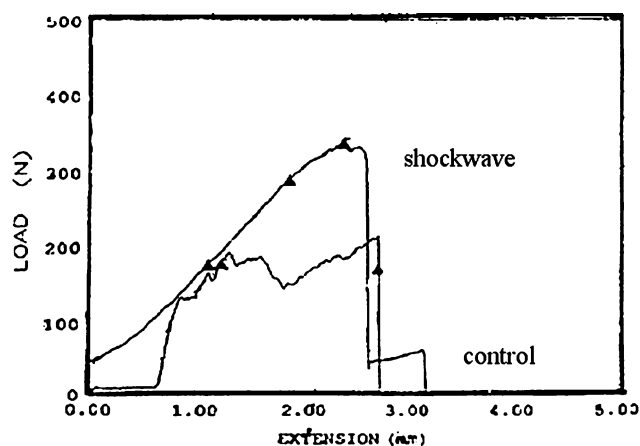


Fig. 2 The load–deflection displacement curves of the bone on slow load compression test performed on MTS machine (Material Testing System). The *upper curve* showed the shockwave group and the control group in the *lower curve*

Histomorphological examination

The harvested bone specimens were fixed in 4% PBS-buffered paraformaldehyde for 48 h and decalcified in PBS-buffered 10% EDTA. Decalcified tissues were embedded in paraffin. Bone specimens were cut longitudinally into 5- μ m thick sections and transferred to poly-lysine-coated slides for conventional hematoxylin-eosin, alcian blue, or alizarin red staining (Sigma Chemicals Inc, St Louis, MO, USA) for the purpose of distinguishing fibrous tissue, cartilaginous, and bony tissues within the specimens.

Immunohistochemical analysis

Sections of the bone specimens were immunostained for VEGF-A, eNOS, PCNA, and BMP-2 (Santa Cruz Biotechnology Inc, CA, USA) to identify angiogenesis and osteogenesis-related growth and proliferating indicators. The immuno-reactivity in specimens was demonstrated using a horseradish peroxidase (HRP)-3', 3'-diaminobenzidine (DAB) cell and tissue staining kit (R&D Systems Inc., Minneapolis, MN, USA). The immuno-activities were quantified from five areas in three sections of the callus site from each animal using a Zeiss Axioskop 2 plus microscope (Carl Zeiss, Gottingen, Germany). All the images of each specimen were captured using a Cool CCD camera (SNAP-Pro cf. Digital kit; Media Cybernetics, Silver Spring, MD, USA). Images were analyzed using an Image-Pro[®] Plus image-analysis software (Media Cybernetics, Silver Spring, MD, USA). The actual number and the percentage of positive immuno-labeled cells over the total cells in each area were counted. An antibody against von Willebrand factor (vWF) was used to identify the immunolocalization of neo-vessels in the callus sites of shockwave and control groups.

Two pathologists blinded to the treatment regimens performed the measurements on all sections.

Statistical analysis

Data were analyzed with a two-way analysis of variance followed by Mann–Whitney *U* test to determine the significance between the shockwave group and the control group. A *P* value of less than 0.05 was considered statistically significant.

Results

Bone strength tests

The results of bone strength including peak load, peak stress, and modulus of elasticity of the shockwave and control groups are summarized in Table 1. All specimens showed a typical load–deflection displacement curve with an initial non-linear response followed by an upward linear slope and a failure response at the time of fracture. The shockwave group showed significantly higher peak load, peak stress, and elastic modulus than the control ($P < 0.05$).

Histomorphological examination

The results of tissue distributions of the shockwave and control groups are summarized in Table 2. The shockwave group showed significantly more cortical bone ($P = 0.048$), less fibrous tissue ($P = 0.053$), and comparable woven bone ($P = 0.116$) as compared to the control (Fig. 3).

Immunohistochemical analysis

Data on the numbers of neo-vessels and positive immunostained cells for VEGF, eNOS, PCNA, and BMP-2 in the callus site of the shockwave and control groups are summarized in Table 3 and illustrated microscopically in

Table 1 The results of biomechanical study

	Control (<i>N</i> = 8)	Shockwave (<i>N</i> = 8)	<i>P</i> value
Peak load (lb)	67.2 \pm 5.7	117.8 \pm 27.5	0.002
Median (range)	68.1 (60.8–77.5)	131.6 (70.9–145.6)	
Peak stress (in-lb)	3.4 \pm 1.4	11.5 \pm 3.4	0.001
Median (range)	3.4 (1.95–5.4)	12.4 (5.9–15.7)	
Modulus of elasticity	18,663 \pm 6,888	71,053 \pm 25,519	0.001
Median (range)	18,332 (9,658–26,788)	71,858 (30,738–112,645)	

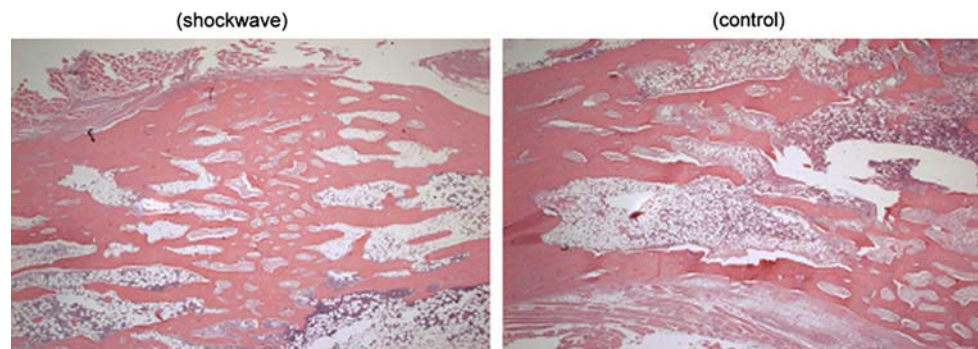
The data were shown in mean \pm SD

P values are based on Mann–Whitney *U* test

Table 2 Tissue distribution in histomorphological examination

	Control (<i>N</i> = 8)	Shockwave (<i>N</i> = 8)	<i>P</i> value
Cortical bone			
Area in mm ² (%)	2,359.0 ± 1,130.5 (45.7 ± 21.9%)	4,054.0 ± 599.0 (67.0 ± 9.9%)	0.006
Median (range)	2,270.4 (1,159–3,540.3)	4,194.9 (3,104.7–4,812.7)	
Woven bone			
Area in mm ² (%)	2,261.0 ± 862.0 (43.8 ± 16.7%)	1,984.7 ± 453.8 (32.8 ± 7.5%)	0.345
Median (range)	2,372.3 (1,048.5–3,348.7)	1,762.5 (1,594–2,738.2)	
Fibrous tissue			
Area in mm ² (%)	188.5 ± 145.0 (17.9 ± 13.8%)	170.1 ± 146.2 (22.3 ± 19.1%)	0.600
Median (range)	128.4 (45.3–439.6)	96.7 (12.3–406.5)	

The data are shown in mean ± SD
P values are based on Mann–Whitney *U* test

Fig. 3 The histomorphological features of the callus site showed more cortical bone, less fibrous tissue and comparable woven bone in shockwave group than the control group**Table 3** The results of immunohistochemical analysis

	Control (<i>N</i> = 8)	Shockwave (<i>N</i> = 8)	<i>P</i> value
Neo-vessels	38 ± 14	68 ± 25	0.037
Median (range)	39 (23–53)	72 (36–96)	
VEGF	158 ± 50	268 ± 53	0.01
Median (range)	174 (75–205)	277 (194–345)	
eNOS	159 ± 41	280 ± 63	0.005
Median (range)	175 (104–195)	294 (195–356)	
PCNA	214 ± 42	301 ± 67	0.02
Median (range)	210 (156–265)	305 (205–402)	
BMP-2	242 ± 91	356 ± 39	0.045
Median (range)	224 (132–385)	367 (312–406)	

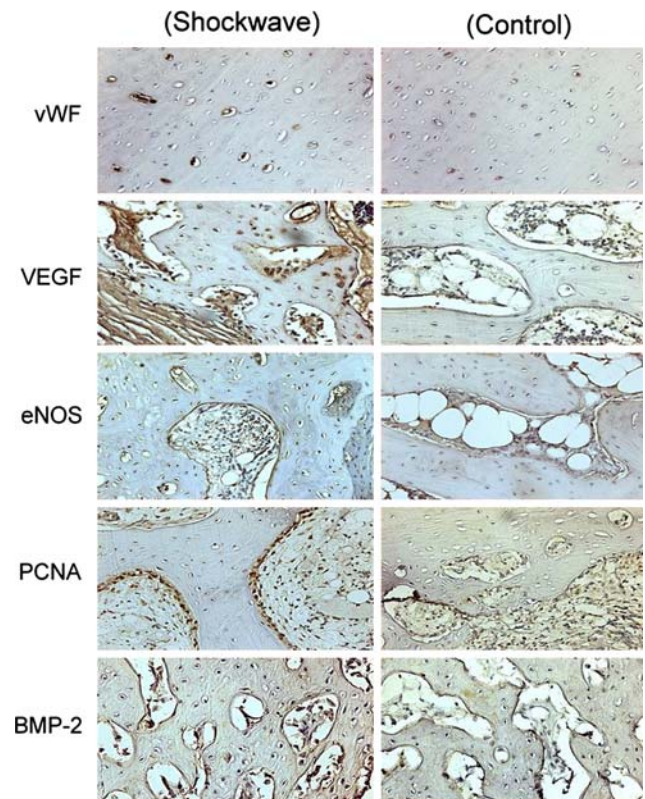
The data represent the total numbers of positive immunostained cells and are shown in mean ± SD

The *P* values are based on Mann–Whitney *U* test

Fig. 4 The shockwave group showed significantly higher numbers of neo-vessels and immuno positive cells including VEGF, eNOS, PCNA, and BMP-2 than the control (*P* < 0.05).

Complications

There was no systemic or local complication including wound infection. There was no device-related problem.

**Fig. 4** The immunohistochemical stains showed significantly higher numbers of neo-vessels (*vWF*) and *VEGF*, *eNOS*, *PCNA* and *BMP-2* in the shockwave group than the control group

Discussion

The exact mechanism of shockwave in bone healing remains unknown. It was speculated that shockwave produced micro-fracture that in turn caused hematoma formation and subsequent callus formation and eventual fracture healing [8]. However, there were insufficient data to scientifically substantiate the theory. The results of the current study demonstrated that ESWT significantly promotes bone healing after fracture.

Many studies investigated the effects of ESWT in bone healing from different elements of experiment including histological examination [2, 6, 7, 15], biomechanical study [22], and molecular biology [1, 16, 18–20, 23]. However, most studies are fragmented and the experiments are focused on single element. Some studies reported that shockwave promoted bone healing primarily by increased cortical bone formation [7, 15]. Other study demonstrated a dose-dependent enhancement of bone mass and bone strength with shockwave treatment [22]. The results of the current study showed that shockwave promoted more cortical bone formation and better bone strength.

Some authors demonstrated that shockwave enhanced pertussis toxin-sensitive bone formation in segmental defect in rats [1]. Others showed that physical shockwaves mediated membrane hyperpolarization and Ras activation for osteogenesis in human bone marrow stromal cells [16], and superoxide mediated shockwave induction of ERK-dependent osteogenic transcription factor (CBFA 1) and mesenchymal cell differentiation toward osteoprogenitors [18, 19, 23]. Another study showed that temporal and spatial expressions of bone morphogenetic protein in extracorporeal shockwave-promoted healing of segmental defect [21]. The results of the current study demonstrated that ESWT-promoted bone healing was associated with increased numbers of neo-vessels and angiogenic and osteogenic growth factors including VEGF, eNOS, PCNA, and BMP-2.

In conclusion, the current study systemically analyzed the biological effects of ESWT in bone healing. ESWT significantly promoted the formation of cortical bone, what might have been associated with increased biomechanical results after fracture in rabbits. Shockwave-promoted bone healing was associated with increases in neovascularization and angiogenic and osteogenic growth factors. It appears that the working mechanism of ESWT in bone healing may be linked to the biological effects as demonstrated in this study.

Acknowledgments Funds were received in total or partial support of the research or clinical study presented in this article. The funding sources were National Health Research Institute (NHRI-EX96-9423EP) and Chang Gung Research Fund (CMRPG8049). The authors thank Ms Yi-Chih Sun, Ya-Ju Yang and Ya-Hsueh Chuang for their

technical assistance in animal experiments and data collection in this study. No benefits in any form have been received or will be received from any commercial party related directly or indirectly to the subject of this article.

References

- Chen YJ, Kuo YR, Yang KD, Wang CJ, Huang HC, Wang FS (2003) Shock wave application enhances pertussis toxin-sensitive bone formation in segmental defect in rats. *J Bone Miner Res* 18:2169–2179
- Delius M, Draenert K, Al Diek Y, Draenert Y (1995) Biological effect of shockwave: in vivo effect of high-energy pulses on rabbit bone. *Ultrasound Med Biol* 21:1219–1225
- Haupt G (1997) Use of extracorporeal shock wave in the treatment of pseudoarthrosis, tendinopathy and other orthopaedic disease. *J Urol* 158:4–11
- Haupt G, Haupt A, Ekkernkamp A, Gerety B, Chvapil M (1992) Influence of shockwave on fracture healing. *Urology* 39:529–532
- Jamsa T, Jalovaara P, Peng Z, Vaananen HK, Tuukkanen J (1998) Comparison of three-point bending test and peripheral quantitative computed tomography analysis in the evaluation of the strength in mouse femur and tibia. *Bone* 23:155–161
- Johannes EJ, Kaulesar Sukul DM, Matura E (1994) High-energy shockwave for treatment of nonunion. An experiment on dogs. *J Surg Res* 57:246–252
- Kaulesar Sukul DM, Johannes EJ, Pierik EG, van Eijck GJ, Kristelijns MJ (1993) The effect of high-energy shock waves focused on cortical bone: an in vitro study. *J Surg Res* 54:46–51
- Ogden JA, Tóth-Kischkat A, Schultheiss R (2001) Principles of shock wave therapy. *Clin Orthop* 387:8–17
- Rompe JD, Rosendahl T, Schöllner C, Theis C (2001) High-energy extracorporeal shock wave treatment of nonunions. *Clin Orthop* 387:102–111
- Schaden W, Fischer A, Sailer A (2001) Extracorporeal shock wave therapy of nonunion or delayed osseous union. *Clin Orthop* 387:90–94
- Schleberger R, Senge T (1992) Noninvasive treatment of long bone pseudoarthrosis by shock waves (ESWL). *Arch Orthop Trauma Surg* 111:224–227
- Valchanou VD, Michailov P (1991) High energy shock waves in the treatment of delayed and nonunion of fractures. *Int Orthop* 15:181–184
- Vogel J, Hopf C, Eysel P, Rompe JD (1997) Application of extracorporeal shock waves in the treatment of pseudoarthrosis of the lower extremity: preliminary results. *Arch Orthop Trauma Surg* 116:480–483
- Wang CJ, Chen HS, Chen CE, Yang KD (2001) Treatment of nonunions of long bone fractures with shock waves. *Clin Orthop* 387:95–101
- Wang CJ, Huang HY, Chen HH, Pai CH, Yang KD (2001) The effect of shock wave therapy on acute fractures of the tibia. A study in a dog model. *Clin Orthop* 387:112–118
- Wang FS, Wang CJ, Huang HC, Chung H, Chen RF, Yang KD (2001) Physical shock wave mediates membrane hyperpolarization and Ras activation for osteogenesis in human bone marrow stromal cells. *Biochem Biophys Res Commun* 287:648–655
- Wang CJ, Huang HY, Pai CH (2002) Shock wave enhanced neovascularization at the bone-tendon junction. A study in a dog model. *J Foot Ankle Surg* 41:16–22
- Wang FS, Wang CJ, Sheen-Chen SM, Chen RF, Kuo YR, Yang KD (2002) Superoxide mediates shock wave induction of ERK-dependent osteogenic transcription factor (CBFA1) and mesenchymal cells differentiation toward osteoprogenitors. *J Biol Chem* 277:10931–10937

19. Wang FS, Yang KD, Chen RF, Wang CJ, Sheen-Chen SM (2002) Extracorporeal shock wave promotes growth and differentiation of bone-marrow stromal cells towards osteoprogenitors associated with induction of TGF-beta1. *J Bone Joint Surg* 84B:457–461
20. Wang CJ, Wang FS, Yang KD, Huang CS, Hsu CC (2003) Shock-wave therapy induced neovascularization at the tendon-bone junction. A study in rabbits. *J Orthop Res* 21:984–989
21. Wang FS, Yang KD, Kuo YR, Wang CJ, Huang HJ, Chen YJ (2003) Temporal and spatial expression of bone morphogenetic proteins in extracorporeal shock wave-promoted healing of fracture defect. *Bone* 32:387–396
22. Wang CJ, Wang FS, Yang KD (2004) Shock wave treatment produced dose-dependent enhancement in bone mass and bone strength after fracture. *Bone* 34:225–230
23. Yang C, Heston WDW, Gulati S, Fair WR (1988) The effects of high-energy shock waves (HESW) on human bone marrow. *Urol Res* 16:427–429